Regulatory cascade involving transcriptional and N-end rule pathways in rice under submergence

Lin, Chih-Cheng; Chao, Ya-Ting; Chen, Wan-Chieh; Ho, Hsiu-Yin; Chou, Mei-Yi; Li, Ya-Ru; Wu, Yu-Lin; Yang, Hung-An; Hsieh, Hsiang; Lin, Choun-Sea; Wu, Fu-Hui; Chou, Shu-Jen; Jen, Hao-Chung; Huang, Yung-Hsiang; Irene, Deli; Wu, Wen-Jin; Wu, Jian-Li; Gibbs, Daniel J; Ho, Meng-Chiao; Shih, Ming-Che

DOI:
10.1073/pnas.1818507116

A Regulatory Cascade Involving Transcriptional and N-end Rule Pathways in Rice under Submergence

Chih-Cheng Lin[1], Ya-Ting Chao[1], Chen Wan-Chieh[1], Hsiu- Yin Ho[1], Mei-Yi Chou[1], Ya-Ru Li[1], Yu-Lin Wu[1], Hung-An Yang[1], Hsiang Hsieh[1], Choun-Sea Lin[1], Fu-Hui Wu[1], Shu-Jen Chou[1], Hao-Chung Jen[1], Yung-Hsiang Huang[1], Deli Irene[1], Wen-Jin Wu[1], Jian-Li Wu[1], Daniel Gibbs[2], Meng-Chiao Ho[1], Ming-Che Shih[1]

[1]Academia Sinica, [2]University of Birmingham

Submitted to Proceedings of the National Academy of Sciences of the United States of America

The rice *SUB1A-1* gene, which encodes a group VII ethylene response factor (ERFVII) plays a pivotal role in rice survival under flooding stress, as well as other abiotic stresses. In *Arabidopsis*, five ERFVII factors play roles in regulating hypoxic responses. A characteristic feature of *Arabidopsis* ERFVIIs is a destabilizing N-terminus, which functions as an N-degron that targets them for degradation via the oxygen-dependent N-end rule pathway of proteolysis, but permits their stabilization during hypoxia for hypoxia-responsive signaling. Despite having the canonical N-degron sequence, SUB1A-1 is not under N-end rule regulation, suggesting a distinct hypoxia signaling pathway in rice during submergence. Herein we show that two other rice ERFVIIs, *ERF66* and *ERF67*, are directly transcriptionally up-regulated by SUB1A-1 under submergence. In contrast to SUB1A-1, ERF66 and ERF67 are substrates of the N-end rule pathway, which are stabilized under hypoxia and may be responsible for triggering a stronger transcriptional response to promote submergence survival. In support of this, overexpression of ERF66 or ERF67 leads to activation of anaerobic survival genes and enhanced submergence tolerance. Furthermore, using structural and protein-interaction analyses, we show that the C-terminus of SUB1A-1 prevents its degradation via the N-end rule and directly interacts with the SUB1A-1 N-terminus, which may explain enhanced stability of SUB1A-1 despite bearing an N-degron sequence. In summary, our results suggest that *SUB1A-1*, *ERF66*, and *ERF67* form a regulatory cascade involving transcriptional and N-end rule control, which allows rice to distinguish flooding from other SUB1A-1-regulated stresses.

submergence | rice | ethylene response factors | transcriptional regulation | N-end rule pathway

Introduction

Floods are climate-related catastrophes that severely influence plant growth, survival, and reproduction. Flooding stress includes waterlogging, when only roots are exposed to soil flooded with water, and submergence, when the shoots are partially or completely immersed in water (1). Under flooding stress, oxygen deprivation prevents aerobic respiration and limits ATP synthesis, resulting in a severe energy crisis (2). The alternative energy supply from NAD^+ regeneration using anaerobic fermentation is not a sufficient strategy, as it accumulates toxic metabolites (3).

Two opposite growth-related flooding survival strategies have evolved in rice: escape and quiescence. The escape strategy is transcriptionally regulated in certain deepwater cultivars by the group VII ethylene response factors (ERFVIIs) SNORKEL1 and 2, and in other varieties through control of gibberellin production by the transcription factor OsEIL1 (4-6). In each of these cases, the rice plant adapts to flooding by promoting internode elongation to grow above the water level, which allows gas exchange with the atmosphere and thus prevents the onset of hypoxia in cells. For the quiescence strategy, a few rice cultivars, such as FR13A, show high tolerance and survive up to two weeks under complete submergence due to the presence of the *SUBMERGENCE 1* (*Sub1*) locus, which consists of a cluster of three *OsERFVIIs* that are related to *SNORKEL1/2* but function differently (5). Among them, *SUB1A-1* functions as a 'master regulator', coordinating the quiescence responses required for survival of prolonged submergence (5). Submergence intolerant cultivars, such as Swarna and IR64, lack *SUB1A-1* or have the *SUB1A-2* allele, which is inactive due to a point mutation within the coding region (5, 7). Introgression or overexpression of *SUB1A-1* into the Swarna and IR64 lines confers significant submergence tolerance (5, 8, 9).

In *Arabidopsis*, five ERFVIIs (*At*ERFVIIs), including HYPOXIA RESPONSIVE ERF (HRE)1, HRE2, RELATED TO APETALA (RAP)2.2, RAP2.3 and RAP2.12 (10), all play some roles in regulating hypoxic responses. Overexpressing individual *AtERFVII* in *Arabidopsis* improves tolerance to hypoxic or flooding stress. Conversely, knockout or knockdown lines of *AtERFVII* genes are more susceptible to flooding stress (11-17). It is proposed that each ERFVII likely has distinct and overlapping targets that orchestrate expression of hypoxia response genes in *Arabidopsis* (18). One characteristic feature of *At*ERFVIIs is a highly conserved N-terminus that starts with the MCGGAI(I/L) motif. *In vitro* and *in vivo* analyses of protein stability showed that this conserved motif functions as an N-degron, which promotes the degradation of ERFVIIs via the oxygen- and nitric oxide (NO)-dependent N-end rule pathway of targeted proteolysis (19-23). In this pathway, methionine aminopeptidase (MetAP) first removes the methionine residue from the N-terminal Met-Cys (Nt-Met-Cys), leaving cysteine as the first residue. Under normoxia, the Nt-Cys residue is subjected to oxygen-dependent oxidation by plant cysteine oxidases (PCOs), which convert Cys to negatively charged Cys-sulfinic acid ($CysO_2$) (24, 25). The Nt-($CysO_2$) is

Significance

Group VII Ethylene response factors (ERFVIIs) function as oxygen sensors via the N-end rule pathway of proteolysis. SUB1A-1, an ERFVII, is a master regulator of submergence tolerance in rice, but escapes the N-end rule pathway, despite containing the canonical N-degron. This raises questions about how rice senses hypoxia stress during submergence. Here, two ERFVIIs, *ERF66* and *ERF67*, are identified as direct transcriptional targets of SUB1A-1 that are substrates of the N-end rule pathway and promote survival of submergence. We propose a regulatory cascade involving *SUB1A-1*and *ERF66*/*ERF67* as a response to submergence stress in rice. Furthermore, we show that the SUB1A-1 C-terminus interacts with the SUB1A-1 N-terminus and prevents its turnover, which may explain how SUB1A-1 evades N-end rule pathway.

Reserved for Publication Footnotes

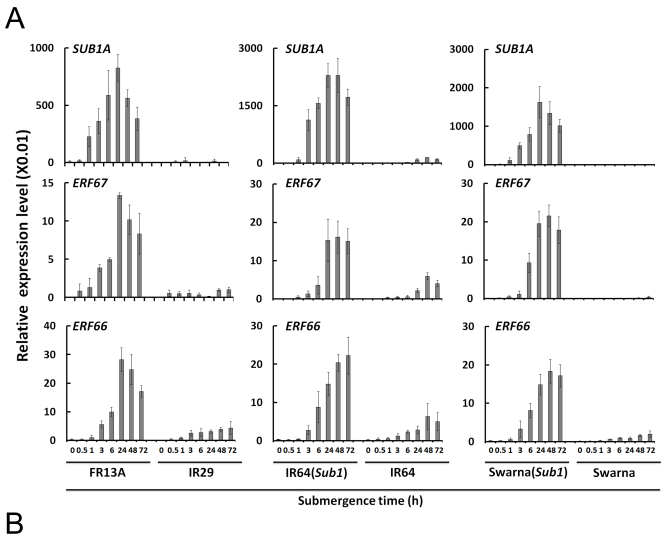

Fig. 1. *Sub1A*, *ERF66* and *ERF67* show similar transcriptional expression patterns during submergence. (A) Transcriptional profiling of SUB1A-1, ERF66 and ERF67 under submergence in FR13A, IR 29, IR64(Sub1), IR64, Swarna(Sub1) and Swarna. Fourteen-day-old seedlings were subjected to submergence treatment and aerial tissues were harvested at indicated time points. Transcript levels of Sub1A, ERF66 and ERF67 were quantified by qRT-PCR. Relative expression level is determined by delta CT of Sub1A, ERF66 and ERF67 normalized by Tubulin mRNA level as the internal control. The data represent means±SD from three independent replicates. (B) N-terminal amino acid sequence alignment of five AtERFVIIs, ERF66, ERF67 and SUB1A-1.

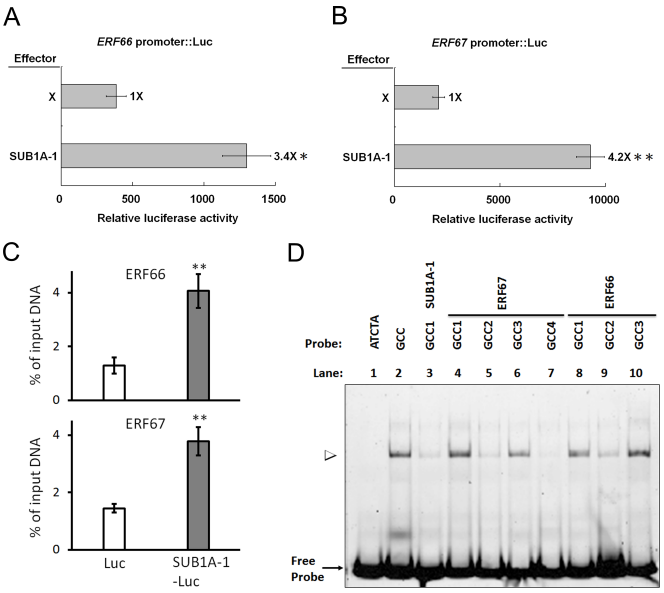

Fig. 2. SUB1A-1 transactivates the *ERF66* and *ERF67* promoters through interacting with GCC boxes.(A) and (B) Trans-activation assay in rice protoplasts showing SUB1A-1-dependent activation of *ERF66* and *ERF67* promoters, respectively.The *SUB1A-1* coding region was linked to the Ubiquitin promoter (UbiP) for use as an effector construct (*SI Appendix*, Fig. S4A). The promoter sequences of ERF66 and ERF67 were fused to the coding sequence of luciferase (Luc) to be used as reporter constructs (*SI Appendix*, Fig. S4A). A *UbiP::GUS* plasmid was used as an internal control. Relative luciferase activity of effector genes (calculated as the ratio of Luc activity/GUS activity/μg total proteins) was then compared with the control. (C) SUB1A-1-Luc-specific enrichment of ERF66/67 promoter sequences using ChIP-qPCR. The data represent mean±SD from three replicates.*, $P<0.05$; **, $P<0.01$ indicate significant difference (Student's *t* test). (D)EMSA assays of the interaction between recombinant SUB1A-1 and FAM-labeled DNA. Each GCC contains different flanking sequence (*SI Appendix*, Fig. S4B and Table S3). In the control experiment (lane 1 & 2), SUB1A-1 has no binding with reference ATCTA probe (65) and binds to reference GCC DNA (66). The ERF67-GCC1, ERF666-GCC10 shows similar binding affinity to SUB1A-1 and SUB1A-1-GCC1, ERF67-GCC2, ERF67-GCC4 and ERF66-GCC2 shows much weaker binding affinity to SUB1A-1 compared to the reference GCC.

then arginylated by arginyl tRNA transferase 1 (ATE1). Lastly, ERFVIIs with Nt-Arg-CysO_2 are proposed to be recognized by the N-recognin E3 ligase proteolysis 6 (PRT6) and degraded via the ubiquitin-proteasome pathway. Under hypoxia, Cys oxidation is limited, which subsequently prevents degradation via the N-end rule pathway, so the *At*ERFVIIs are stabilized and accumulate to transcriptionally trigger downstream hypoxic responses.

In contrast to *Arabidopsis*, the rice genome consists of 18 *ERFVIIs*, some of which are cultivar-specific, such as *SUB1A-1* and *SNORKEL1/2*. *SUB1A-1* and *SNORKEL1/2* play key regulatory roles in FR13A and deepwater rice, respectively, in response to flooding stress (4, 5, 10). The involvement of *AtERFVIIs* and *SUB1A-1* in activating hypoxic responsive and fermentative genes during submergence suggests that they have similar functions as 'master regulators' of hypoxic responses in *Arabidopsis* and rice, respectively. However, ectopic expression of SUB1A-1 in *Arabidopsis* cannot enhance tolerance to submergence in the dark (26). Despite possessing a similar Met-Cys-initiating N-terminal degron sequence to the *At*ERFVIIs, SUB1A-1 is not subject to regulation by the N-end rule pathway *in vitro* (19). The ability of SUB1A-1 to escape degradation through the N-end rule pathway may be key to its involvement in other abiotic stress responses, such as surviving reactive oxygen species accumulation and rapid dehydration following de-submergence, and prolonged darkness (27, 28). It is generally believed that SUB1A-1 may serve a key signaling hub that regulates responses to various stresses independently of oxygen levels. This raises two critical questions: 1) How is oxygen sensing regulated in rice; and 2) How does SUB1A-1 escape N-end rule regulation?

Herein, we report that two rice ERFVIIs, *ERF66* and *ERF67*, function downstream of SUB1A-1 to form a regulatory cascade in response to submergence stress. *ERF66* and *ERF67* are induced under submergence in a SUB1A-1-dependent manner, and are direct transcriptional targets of SUB1A-1. In contrast to SUB1A-1, ERF66 and ERF67 are both subjected to oxygen-dependent turnover via the N-end rule pathway. Overexpression of GST-tagged ERF66/67 in the submergence-sensitive TNG67 cultivar resulted in enhanced expression of genes associated with submergence tolerance, and increased submergence survival. NMR structural analysis of the SUB1A-1 N-terminus revealed a flexible, random coil structure that should permit interaction with N-end rule enzymatic components and therefore degradation. However, we found that the C-terminal region of SUB1A-1 prevent its degradation and directly interacts with the SUB1A-1 N-terminus, providing new insight into how SUB1A-1 evades degradation under hypoxia. Taken together, we propose that the flooding response in SUB1A-1-encoding cultivars involves SUB1A-1-dependent transcriptional activation of ERF66 and ERF67, which are then stabilized only under hypoxia to coordinate the submergence-specific response, thus allowing rice plants to discriminate flooding from other SUB1A-1 regulated stresses.

Results

SUB1A-1 regulates *ERFVII* gene expression during submergence

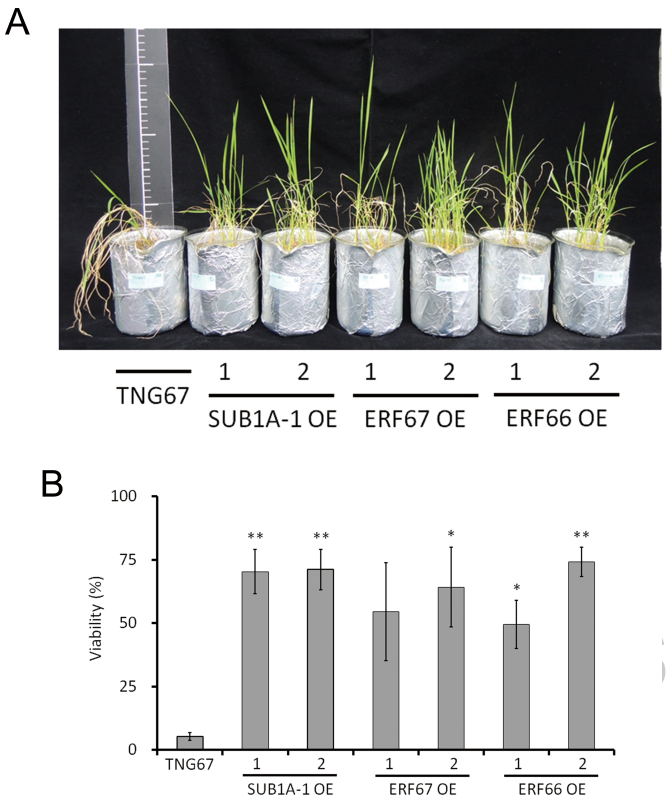

Fig. 3. Phenotypes of SUB1A-1, ERF67 and ERF66 overexpression lines after submergence. (A) Rice plants after 14 days of recovery from submergence. 14-day-old rice plants were submerged for 7 days in dark. After submergence, plants were returned to normal growth conditions for 14 days of recovery and photographed. (B) Viability of whole plants after de-submergence. The whole plant viability of each genotype was evaluated in the samples shown in (A). Plants were scored as viable if a new leaf appeared during the recovery period. The data represent means±SD from two independent replicates. *, $P<0.05$; **, $P<0.01$ indicate significant difference (Student's *t* test). The *P* value of ERF67 OE Line 1 is 0.06.

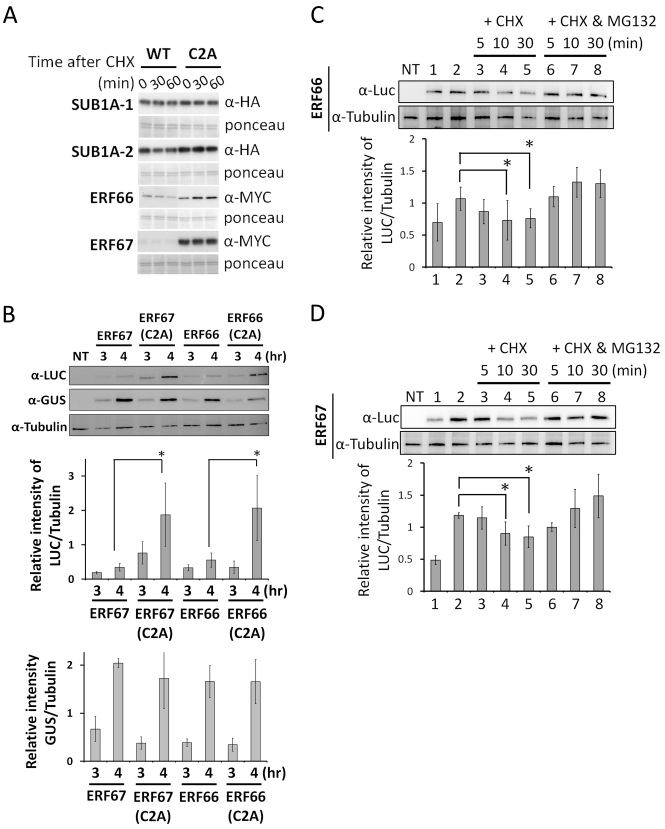

Fig. 4. ERF66 and ERF67 are substrates of the N-end rule pathway. (A) *In vitro* analysis of protein stability of HA or MYC-tagged wild-type and C2A variants of SUB1A-1, SUB1A-2, ERF66 and ERF67 following treatment with CHX. (B) The stability of ERF66 and ERF67 expressed in rice protoplasts is enhanced by a C2A mutation or treatment with MG132. *UbiP::ERFVII-Luc* constructs were co-transfected into TNG67 rice protoplasts with a *UbiP::GUS* plasmid, which was used as a stable control. The transfected protoplasts were incubated in W5 solution for 3 or 4 hr then harvested for western blot analysis (*SI Appendix*, Fig. S7A), and the relative levels of Luc and GUS were normalized to tubulin, respectively. NT: Non-transfected. The molecular weights of ERF66/67-Luc fusion proteins are approximately 87/85 kDa, respectively. (C) and (D) The CHX chase of ERF66 and ERF67 with/without MG132 in rice protoplasts. The protein levels of ERF66/ERF67 4 hr after transformation without MG132 (lane 1) and with MG132 (lane 2) are shown. CHX chase experiments were initiated after 4h treatment with MG132 to ensure high levels of protein at the beginning of the chase, by replacing buffer with either CHX only (100 μM) or CHX and MG132 (20 μM). The relative levels of Luc were normalized to tubulin. The data represent means±SD from three independent replicates. *, $P<0.05$ indicates significant difference (Student's *t* test).

To understand the transcriptional networks regulated by SUB1A-1 during submergence, we dissected the transcriptional profiles of 16 *OsERFVIIs* (all except *SNORKEL1* and *2,* which are absent in most cultivars) in two *Indica* rice cultivars that display contrasting sensitivity toward submergence stress. FR13A, the submergence-tolerant cultivar, possesses the tolerant *SUB1A-1* allele. IR29, the submergence-sensitive cultivar, possesses the intolerant *SUB1A-2* allele, which contains an inactive SUB1A-2 due to a single amino acid substitution at position 186 from serine (SUB1A-1) to proline (SUB1A-2) (5, 7). By comparing the results of qRT-PCR (*SI Appendix*, Fig. S1), we found that the transcript levels of *ERF59*, *ERF60*, *ERF61*, *ERF66* and *ERF67* were much higher under submergence in FR13A than in IR29. It is reported that ERF73/SUB1C is negatively regulated by SUB1A-1 (5, 8). Consistently, our result shows the transcript level of *ERF73/SUB1C* was much lower in FR13A than in IR29 (*SI Appendix*, Fig. S1). In order to eliminate the difference in transcriptional levels that arise from different genetic backgrounds, we then compared *OsERFVII* expression profiles of submergence-sensitive cultivars, IR64 and Swarna, with those of corresponding near-isogenic lines with introgressed *SUB1A-1*. The results showed that only the transcripts of *ERF66* and *ERF67* were significantly more abundant in the *SUB1A-1* introgressed cultivars IR64(*Sub1*) and Swarna(*Sub1*) than in submergence-sensitive IR64 and Swarna (Fig. 1A and *SI Appendix*, Figs. S2 and S3). Jung et al. previously found that *ERF66*, *ERF67,* and *ERF68* were induced in the *Sub1* near-isogenic line of M202 using microarray approaches (29). Our results also showed that *ERF68* responds to submergence within 30 minutes but we found no differences in *ERF68* expression between wild-type cultivars and corresponding SUB1A-1 lines (*SI Appendix*, Figs. S1-S3). In contrast, our data showed that *ERF66* and *ERF67* are up-regulated only in the presence of SUB1A-1 upon submergence (Fig. 1A).

SUB1A-1 directly activates *ERF66* and *ERF67*

Next we used protoplast transient assays to examine whether SUB1A-1 directly controls the transcription of *ERF66* and *ERF67* genes. Using an effector construct encoding SUB1A-1 driven by the *Ubiquitin* promoter (UbiP), co-transformed with a reporter construct encoding luciferase driven by the *ERF66* promoter (*SI Appendix*, Fig. S4A), we found a 3- to 4-fold increase in luciferase activity compared to the control (Fig. 2A). Similarly, SUB1A-1 stimulated transcription from the *ERF67* promoter 4- to 5-fold (Fig. 2B). These results show that SUB1A-1 transcriptionally

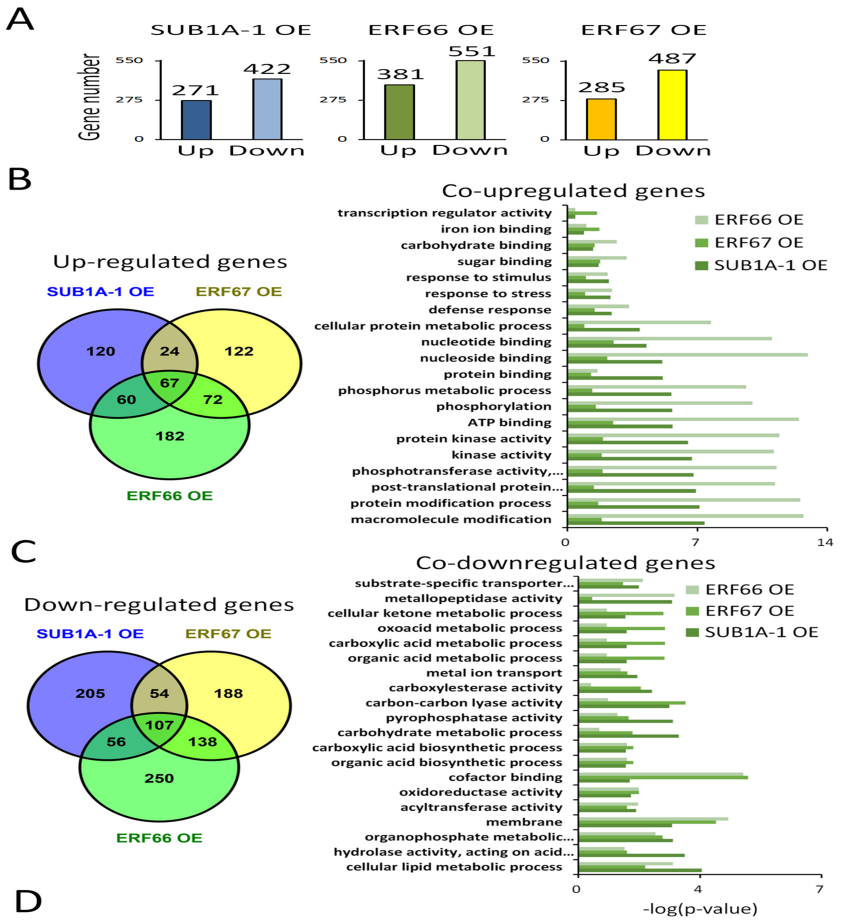

TNG67	SUB1A-1 OE	ERF67 OE	ERF66 OE	MSU ID	Description
1.76	2.51	2.07	4.27	LOC_Os03g13140	Non-symbiotic hemoglobin 1 (rHb1) (ORYsa GLB1a).
1.15	2.33	2.76	4.54	LOC_Os03g12510	Non-symbiotic hemoglobin 2 (rHb2) (ORYsa GLB1b).
0.91	1.30	1.47	1.65	LOC_Os11g10480	Alcohol dehydrogenase 1.
0.43	1.53	0.71	2.32	LOC_Os11g10510	Alcohol dehydrogenase 2.
0.75	1.42	0.86	1.78	LOC_Os08g03420	Galactose oxidase/HUP6-like gene.
0.96	1.17	2.27	1.86	LOC_Os02g07730	Dreg-2 like protein/haloacid dehalogenase-like hydrolase domain-containing protein 3
0.82	1.08	1.04	1.25	LOC_Os05g44922	Phosphofructokinase 5.
-0.90	3.71	2.92	4.01	LOC_Os08g42750	Similar to Calcium-dependent protein kinase.
0.56	2.56	3.94	4.70	LOC_Os03g62480	UDP-glucuronosyl/UDP-glucosyltransferase family protein.
1.16	2.51	2.54	2.80	LOC_Os11g43530	Similar to Glutaredoxin-C13.
1.15	2.33	2.76	4.54	LOC_Os03g12510	Non-symbiotic hemoglobin 2 (rHb2) (ORYsa GLB1b).
1.42	2.27	2.38	2.41	LOC_Os03g07140	Similar to Male sterility protein 2.
0.78	1.75	2.31	2.21	LOC_Os03g49524	UDP-glucuronosyl/UDP-glucosyltransferase family protein.
-0.88	1.64	4.53	1.19	LOC_Os09g09540	Zinc finger, SWIM-type domain containing protein.
0.44	1.59	1.15	1.19	LOC_Os02g30780	Glycosyl transferase, family 31 protein.
0.80	1.41	2.53	1.91	LOC_Os11g40480	Kelch related domain containing protein.
0.30	1.16	1.32	1.27	LOC_Os01g43950	Helix-loop-helix DNA-binding domain containing protein.

Fig. 5. Transcriptomic analyses of SUB1A-1, ERF66 and ERF67 overexpression lines under submergence. (A) Histogram showing numbers of up- and down-regulated genes (>2-fold, $P<0.05$) in SUB1A-1/ERF67/ERF66 overexpression lines that are not differentially regulated in TNG67. (B) Overlap among genes significantly up-regulated by overexpressing SUB1A-1, ERF66 and ERF66, and distribution of functional categories of up-regulated genes. (C) Overlap among genes significantly down-regulated by SUB1A-1, ERF66 and ERF67, and distribution of functional categories of down-regulated genes. Histograms in (C) and (D) indicate *P* values of the enriched functional categories. (D) Representative genes are up-regulated in SUB1A-1 and ERF66/67 overexpression lines. The first 7 genes are orthologous of core hypoxia genes, which are up-regulated in SUB1A-1 and ERF66/67 overexpression lines.

activates the *ERF66* and *ERF67* genes. We then confirmed the direct binding of SUB1A-1 with the *ERF66/67* promoter region by ChIP-qPCR (Fig. 2C and *SI Appendix*, Fig. S4B), observing a 2- to 3-fold enrichment of *ERF66* and *ERF67* promoter sequences in SUB1A-1 immunoprecipitate compared to the control.

The conserved APETALA2 (AP2) domain of ERFVIIs is known to interact with a GCC box with a core sequence GCCGCC (30-32). Multiple-GCC boxes with various flanking sequence are found in *ERF66* and *ERF67* promoters and one is found in *SUB1A-1* promoter (*SI Appendix*, Fig. S4B). Our EMSA assays using recombinant SUB1A-1 show SUB1A-1 preferably interacts with ERF66-GCC1, ERF66-GCC3, ERF67-GCC1 and ERF67-GCC3, but not SUB1A-1-GCC1 or other GCC boxes in the promoters of *ERF66* or *ERF67* (Fig. 2D). To eliminate the possibility that the fluorescent probe may interfere with the binding, we confirmed our findings with competition assays using unlabeled GCC boxes (*SI Appendix*, Fig. S4C). In a more recent study, RAP2.2 and RAP2.12 could bind to an extended GCC consensus sequence, designated the *Arabidopsis* hypoxia-responsive promoter element (HRPE), to activate core hypoxia response genes in *Arabidopsis* (33). Our EMSA results extend the current knowledge by demonstrating that the flanking sequence of the GCC boxes in the promoters of *ERF66* and *ERF67* is also important and may play roles in SUB1A-1 selectivity for transcriptional activation.

Together, our experiments (Figs. 1 and 2) show that SUB1A-1 directly up-regulates *ERF66* and *ERF67* in response to submergence through interacting with GCC boxes in their respective promoter regions.

Overexpression of ERF66, ERF67 or SUB1A-1 enhances submergence tolerance in transgenic rice

Since *ERF66* and *ERF67* are downstream targets of SUB1A-1, we next examined if ERF66 and ERF67 participate in submergence tolerance. We individually overexpressed each gene (*SI Appendix*, Fig. S5) in the submergence-sensitive TNG67 cultivar (which does not contain *SUB1A-1*) and assessed viability of the

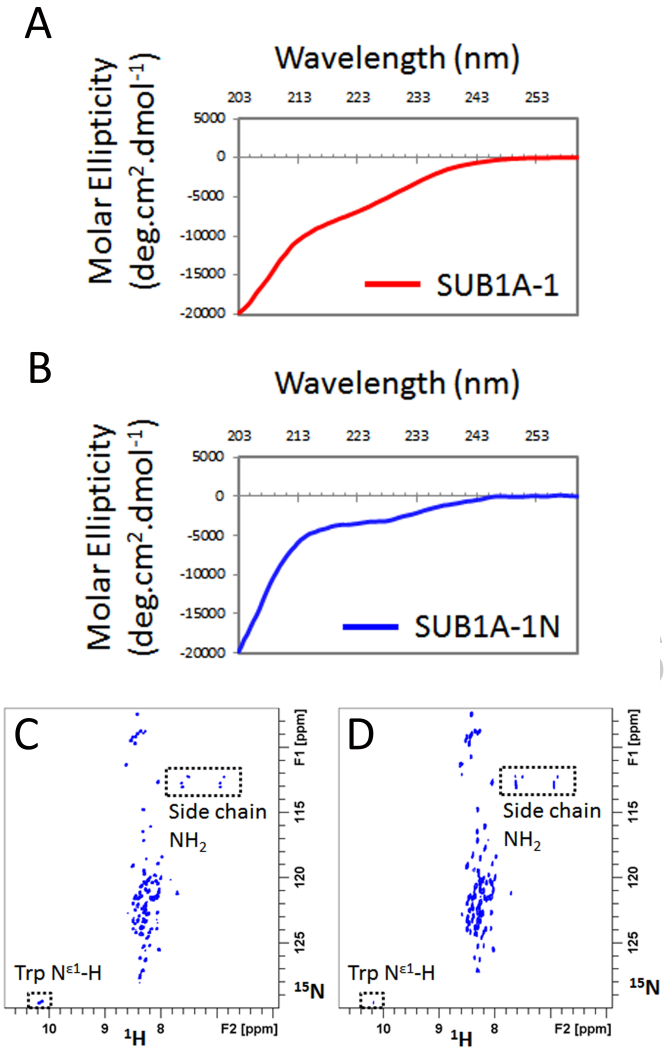

Fig. 6. The CD and NMR spectra of recombinant SUB1A-1 constructs.CD spectra of full length SUB1A-1 (A) and SUB1A-1 N-terminus only (B) shows that SUB1A-1 and its N-terminus are mostly unstructured. The cross peaks of 2D $^{1}H,^{15}N$-BEST-HSQC spectrum of SUB1A-1 N-terminus only (C) occur in a very narrow chemical shift range, indicating a random coil structure when it combines with the CD result. The solvent exposed amide proton 2D $^{1}H,^{15}N$-HSQC spectrum of SUB1A-1 N-terminus only. (D) shows that most of the amide protons have exchange cross peaks with water, indicating that amide are solvent exposed.

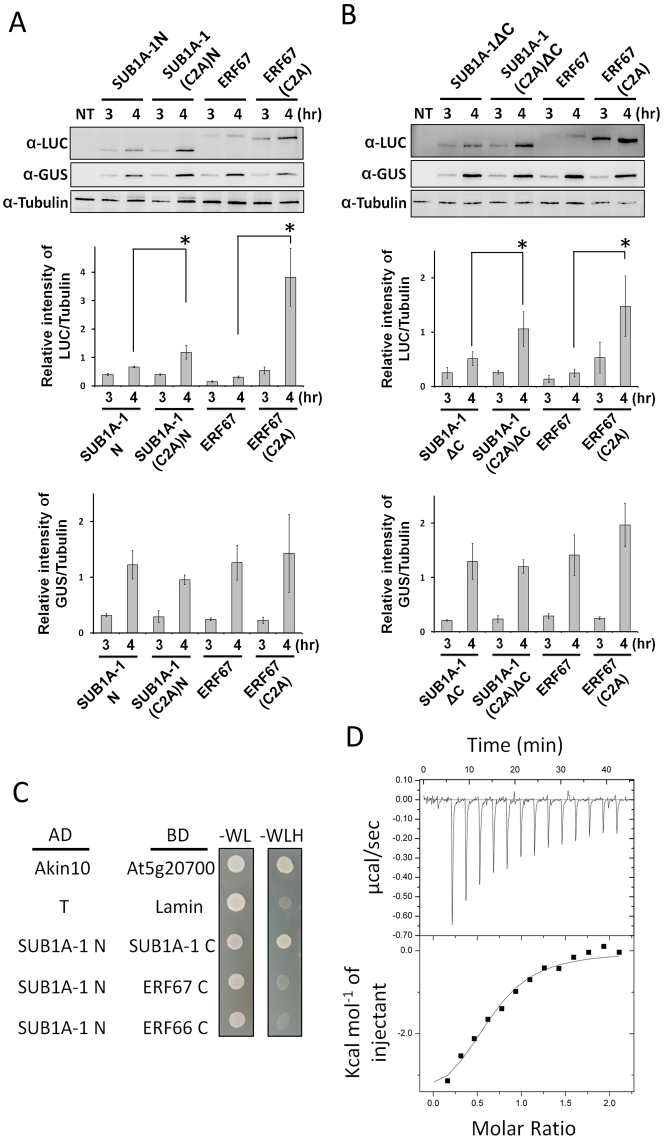

Fig. 7. C-terminally-truncated SUB1A-1 can be degraded by the N-end rule pathway. Western blot analysis of proteinstability of the truncated SUB1A-1 in TNG67 rice protoplasts. (A) and (B) Protein stability assays of SUB1A-1N and SUB1A-1ΔC, respectively. *UbiP::SUB1A-1N/SUB1A-1ΔC/ERF67-Luc* constructs were co-transfected into TNG67 rice protoplasts with a *UbiP::GUS* plasmid, which was used as a stable control. The transfected protoplasts were incubated in W5 solution for 3 or 4 hr then harvested for further western blot analyses and the relative levels of Luc and GUS were normalized to tubulin, respectively. NT: Non-transfected. The data represent means±SD from three independent replicates. *, $P<0.05$ indicates significant difference (Student's *t* test). The molecular weight of SUB1A-1N/SUB1A-1ΔC-Luc fusion proteins are approximately 74/81 kDa, respectively. The molecular weight of the ERF67-Luc fusion protein is approximately 85 kDa. (C) Yeast two-hybrid assay testing interactions between the SUB1A-1 N-terminus and SUB1A-1, ERF66 or ERF67 C-termini. AD, GAL4 activation domain; BD, GAL4 DNA binding domain. Positive interactions are represented by growth on the triple-dropout medium (-WLH), which test for expression of the *HIS3* reporter gene. Yeast growth on the double-dropout medium (-WL) is included as a co-trasnformation control. (D) iTC experiment for the binding between SUB1A-1 N- and C-termini. The upper curve shows corrected heat pulses resulting from titration of SUB1A-1 C-terminus and the lower graph shows the integrated heat pulse along with a fit.

resulting transgenic lines following 7 days of submergence. Using two independent lines for each transgene, we found that all three transcription factors, including SUB1A-1, individually led to enhanced submergence tolerance compared to the wild-type (Fig. 3). In contrast to Xu et al (2006) (5) we did not observe a semi-dwarf phenotype in the TNG67 SUBA-1 OE lines, which may be related to the use of different genetic backgrounds in the two studies.

ERF66 and ERF67 are subject to N-end rule regulation

SUB1A-1, ERF66 and ERF67 all have the conserved N-degron sequence of MCGG (Fig. 1B and *SI Appendix*, Fig. S6), but SUB1A-1 is not subjected to N-end rule regulation *in vitro* (19). We next investigated if ERF66 and ERF67 are targets of the N-end rule pathway. Using a previously established *in vitro* assay (19), where proteins are expressed in a rabbit reticulocyte system containing conserved N-end rule components, we showed that a cysteine to alanine mutation at residue position 2 (C2A) in ERF66-MYC and ERF67-MYC led to enhanced protein stability in presence of cycloheximide (CHX; protein synthesis inhibitor) compared to the wild-type, whereas wild-type and C2A-variants of SUB1A-1-HA showed no difference in protein stability (Fig.

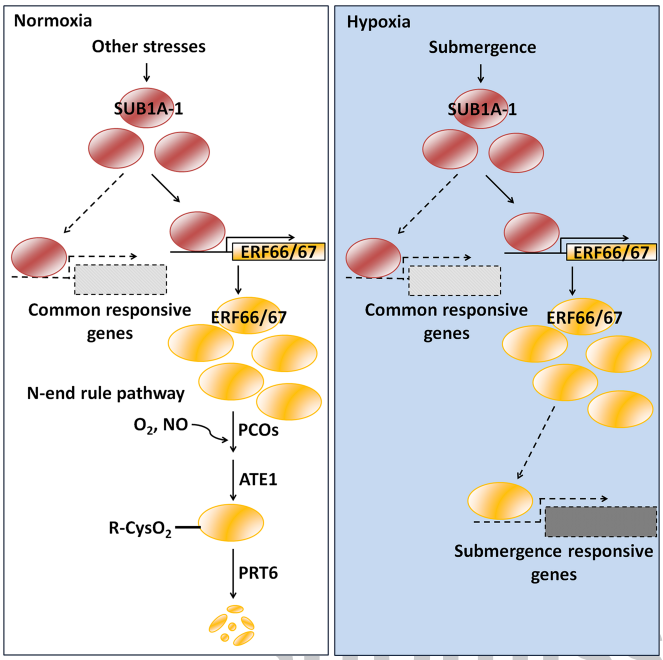

Fig. 8. Model of the regulatory cascade of *SUB1A-1*, *ERF66* and *ERF67* that involves transcriptional and N-end rule pathways in response to submergence stress in submergence-tolerant rice cultivars.

4A). Since N-terminal Cysteine is crucial for turnover of *Arabidopsis* ERFVIIs (19, 20), these *in vitro* data suggest that ERF66 and ERF67, in contrast to SUB1A-1, are substrates of the N-end rule pathway.

We next examined the regulation of ERF66, ERF67 and SUB1A-1 stability *in vivo*, by transiently expressing C-terminally Luc tagged WT and C2A mutant variants driven by the *Ubi* promoter in TNG67 rice protoplast cells (Fig. 4B and *SI Appendix*, Fig. S7A and S7B). Here we could only detect low levels of wild-type ERF66/67 by western blot, but either a C2A mutation or treatment with MG132 led to enhanced accumulation (Fig. 4B-4D). In contrast, WT and C2A variants of SUB1A-1 accumulated to similar levels (*SI Appendix*, Fig. S7C). Following treatment with CHX, the accumulated WT ERF66/67-Luc proteins were degraded over time, but showed enhanced stability in presence of MG132, confirming that observed differences in ERF66/67 levels are linked to their regulation via proteasome degradation pathway (Fig. 4C and 4D). We also examined the influence of submergence-induced hypoxia on ERF66 and ERF67 stability using a transgenic *Arabidopsis* approach. Here we observed increased protein levels of GFP-tagged ERF66 and ERF67 during a submergence time course (*SI Appendix*, Fig. S8A), while transcript change remained relatively constant compared to the hypoxia-inducible control gene *ALCOHOL DEHYDROGENASE1* (*ADH1*) (*SI Appendix*, Fig. S8B). This indicates that submergence-induced hypoxia leads to ERF66 and ERF67 stabilization, similar to *Arabidopsis* ERFVIIs. Collectively, our protein stability assays reveal that both ERF66 and ERF67 are substrates of the N-end rule pathway, whilst SUB1A-1 is not.

***ERF66/ERF67* and *SUB1A-1* form a signaling cascade to regulate downstream submergence responses**

It is reported that *SUB1A-1* could be activated by different abiotic stresses. We showed that *ERF66* and *ERF67* act genetically downstream of *SUB1A-1* and are subjected to N-end rule regulation during hypoxia. Hence, we speculated that there are two sets of genes, one regulated by the SUB1A-1 and *ERF66/ERF67* cascade, and the other regulated solely by SUB1A-1. We carried out an RNA-seq analysis of SUB1A-1 (line 1), ERF66 (line 2) and ERF67 (line 2) transgenic lines (as used in Fig. 3) to examine the effect of overexpressing these transcription factors on global gene expression (see *SI Appendix*, Dataset S1 for full results). In these analyses we first normalized expression levels after 24-hr treatment of submergence with corresponding expression levels at 0-hr treatment, and then eliminated any changes observed in the submergence-sensitive TNG67 background line. In doing so, we identified 271, 285, and 381 genes that were more than 2-fold up-regulated in the SUB1A-1-, ERF67- and ERF66- individual overexpression lines, respectively, but not in TNG67. Interestingly, *ERF66* and *ERF67* were about 3- and 30-fold up-regulated in SUB1A-1 overexpression line, respectively. Furthermore, 422, 487 and 511 genes were more than 2-fold down-regulated in the SUB1A-1-, ERF67- and ERF66- individual overexpression line, respectively (Fig. 5A). Analysis of the gene lists revealed two distinct groupings of differentially expressed genes, one that is dependent on SUB1A-1 with ERF66 and/or ERF67, and the other that is regulated solely by SUB1A-1 (Fig. 5B and 5C). For the first group, Venn diagram analyses show 151 genes in total were up-regulated in SUB1A-1 and ERF67 (24 genes), SUB1A-1 and ERF66 (60 genes), and all three individual overexpression lines (67 genes), indicating that ERF66 and ERF67 may have different downstream targets (Fig. 5B). Meanwhile, we also found 217 gene in total were down-regulated in SUB1A-1 and ERF67 (54 genes), SUB1A-1 and ERF66 (56 genes), and all three individual overexpression lines (107 genes) (Fig. 5C).

A Gene Ontology (GO) analysis revealed that up-regulated genes were involved in diverse processes, including response to stress, defense response, phosphorylation, and protein kinase activity (Fig. 5B), whilst downregulated genes included those associated with carbohydrate metabolic process, cellular lipid metabolic process (Fig. 5C). The up-regulated genes across all three transgenic lines included orthologues of core hypoxia-related genes, including non-symbiotic hemoglobin 1/2 (LOC_Os03g13140/LOC_Os03g12510), alcohol dehydrogenase 1/2 (LOC_Os11g10480/LOC_Os11g10510), Galactose oxidase/HUP6-like gene (LOC_Os08g03420), Dreg-2 like protein/haloacid dehalogenase-like hydrolase domain-containing protein 3 (LOC_Os02g07730) and phosphofructokinase 5 (LOC_Os05g44922) (Fig. 5D and *SI Appendix*, Dataset S1). This provides a transcriptional explanation for the enhanced submergence tolerance of these overexpression lines (Fig. 3), and further confirms the involvement of all three ERFVIIs in coordinating submergence responses.

The N-terminus of SUB1A-1 has random coil structure

The key enzymes in the N-end rule pathway, including MetAP, ATE and PRT6, are highly conserved in eukaryotes (22, 23). The active binding site of the human PRT6 functional homologue, UBR1, is a shallow and mostly hydrophobic pocket into which activated N-degrons can fit (34, 35). To understand how SUB1A-1 might evade N-end rule regulation, despite having an N-terminal motif similar to the AtERFVIIs and OsERF66/67, we used circular dichroism (CD) and nuclear magnetic resonance (NMR) spectroscopy to examine recombinant SUB1A-1 and SUB1A-1 N-terminus (SUB1A-1N), which consists of the first 115 amino acids of SUB1A-1 (*SI Appendix*, Fig. S9) with an additional N-terminal serine (the residue of TEV protease cleavage site) and C-terminal His-tag for protein production and purification purpose. The secondary structure investigation by CD revealed that the full-length SUB1A-1 is mostly unstructured, and SUB1A-1N also resembles a random coil (Fig. 6A and 6B). We further analyzed the structural properties of SUB1A-1N by nuclear magnetic resonance (NMR) spectroscopy. As shown in Fig. 6C, the 2D $^{1}H^{15}N$-BEST-HSQC spectrum shows that the cross peaks of the backbone N-H groups of SUB1A-1N occur in a very narrow chemical shift range, indicative of a random coil

structure when combining this result with its random coil CD curve. Furthermore, the solvent exposed amide proton 2D $^{1}H^{15}N$-HSQC spectrum of SUB1A-1N shows that most of the amide protons have exchanged cross peaks with water (with an exchange rate greater than 3 Hz), indicating that backbone amides are solvent exposed, and are not protected by structure or hydrogen-bonds (Fig. 6D). The combined CD and NMR analyses therefore indicate that SUB1A-1N is unstructured, suggesting that the N-terminus of SUB1A-1 is very flexible and should be recognized by components of N-end rule. This raises the possibility that other regions of the SUB1A-1 might be involved in preventing degradation by the N-end rule pathway, or that other proteins bind to SUB1A-1 to shield the N-degron.

The C-terminus of SUB1A-1 prevents its degradation by the N-end rule pathway

To test whether other regions of SUB1A-1 might interfere with its degradation by the N-end rule, we analyzed the protein stability of two C-terminally truncated variants of SUB1A-1 in TNG67 rice protoplast, including: (1) SUB1A-1N (SUB1A-1 N-terminus only) and (2) SUB1A-1ΔC (the SUB1A-1 lacking the C-terminus) (*SI Appendix*, Fig. S7B). The protein levels of SUB1A-1N and SUB1A-1ΔC were similar to wild-type ERF67 but significantly lower than ERF67(C2A), indicating that truncated SUB1A-1 is unstable after removing the C-terminus (Fig. 7A and 7B). To confirm that this instability is due to degradation via the N-end rule pathway, we transiently expressed C2A variants (*SI Appendix*, Fig. S7B) of both truncation constructs in TNG67 rice protoplast cells. The protein quantities of SUB1A-1(C2A)N and SUB1A-1(C2A)ΔC were much higher than SUB1A-1N and SUB1A-1ΔC, and similar to ERF67(C2A) (Fig. 7A and 7B). This suggests that, in contrast to full length SUB1A-1 (*SI Appendix*, Fig S7C), C-terminally truncated variants of SUB1A-1 are degraded via N-end rule pathway. To understand how the SUB1A-1 C-terminus interferes with SUB1A-1 degradation, we examined the capacity for these two regions of SUB1A-1 to interact with each other. Yeast two-hybrid analysis revealed an interaction between the SUB1A-1 N-terminus and C-terminus (Fig. 7C). This was specific for the SUB1A-1 C-terminus, since ERF66 and ERF67 C-termini did not interact with the SUB1A-1 N-terminus. This interaction was also confirmed by isothermal Titration Calorimetry (iTC) experiments using recombinant SUB1A-1 N-terminus and C-terminus (Fig. 7D). Thus we propose that the C-terminal region of SUB1A physically interacts with the SUB1A-1 N-terminus, and that this shields the N-degron, preventing protein turnover.

Discussion

ERFVII transcription factors are involved in hypoxia-sensing and regulating responses to flooding and/or hypoxic stress. For example, all five ERFVIIs in *Arabidopsis* function as important regulators of flooding and/or hypoxia tolerance, whilst ERFVIIs in barley, *Rumex* and *Rorippa* regulate the response to waterlogging (12, 15, 17, 29, 36-40). Furthermore, *Arabidopsis* ERFVIIs have also been linked to other abiotic and biotic responses (12, 41-43). In rice, the ERFVII SUB1A-1 is the master regulator of the quiescence submergence-survival response, as well other abiotic stresses (27, 28). However, in contrast to all other investigated ERFVIIs, SUB1A-1 was shown to resist the N-end rule pathway, suggesting it is not directly involved in hypoxia sensing. In addition, SUB1A-1 does not confer flooding tolerance in *Arabidopsis*, suggesting some degree of difference between rice and *Arabidopsis* quiescence mechanism in response to submergence stresses. Here, we propose a novel regulatory cascade in the *SUB1A-1*-dependent submergence response that involves two other rice *ERFVIIs*, *ERF66* and *ERF67*.

We dissected the transcriptional kinetics of 16 *OsERFVIIs* in two *indica* cultivars (submergence-tolerant FR13A and submergence-sensitive IR29), and found that many are transcriptionally upregulated in response submergence treatment (*SI Appendix*, Fig. S1). This includes ERF70, which was recently shown to contribute to improved recovery from submergence stress (44). Five of these *OsERFVIIs* (*ERF59*, *ERF60*, *ERF61*, *ERF66* and *ERF67*) had higher transcript levels in FR13A than in IR29, and their expression patterns were similar to those of *SUB1A-1* in FR13A and IR29 (*SI Appendix*, Fig. S1). By cross-examining the transcript levels of these five *ERFVIIs* in other submergence-tolerant cultivars, IR64(*Sub1*) and Swarna(*Sub1*), and other sensitive cultivars, IR64 and Swarna, we found that only *ERF66* and *ERF67* showed enhanced transcript abundance in tolerant cultivars than in sensitive cultivars (Fig. 1), indicating that they are downstream targets of SUB1A-1 during submergence.

Using *trans*-activation assays, we found that SUB1A-1 could transcriptionally activate *ERF66* and *ERF67* (Fig. 2A and 2B). We also confirmed that SUB1A-1 can interact with *ERF66* and *ERF67* promoter by ChIP-qPCR (Fig 2C). Multiple GCC boxes with different flanking sequences in the promoter regions of *ERF66* and *ERF67* are identified (*SI Appendix*, Fig. S4B) and our EMSA studies showed that recombinant SUB1A-1 selectively binds to several (but not all) of the identified GCC boxes (Fig. 2D and *SI Appendix*, Fig. S4C). Collectively, our data suggest that SUB1A-1 directly up-regulates *ERF66* and *ERF67* via interaction with GCC boxes in their promoters, and *ERF66* and *ERF67* are therefore downstream targets of SUB1A-1. Moreover, overexpression of ERF66 or ERF67 in the TNG67 submergence-sensitive cultivar led to enhanced submergence-tolerance (Fig. 3).

By performing protein stability studies (Fig. 4 and *SI Appendix*, Figs. S7 and S8), we showed that ERF66 and ERF67, but not SUB1A-1 (19), are substrates for the N-end rule pathway, despite all three proteins having canonical N-degron sequences in their N-termini. The NMR analyses showed that the N-terminus of SUB1A-1 is a random coil structure (Fig. 6), indicating that the N-terminus of SUB1A-1 is very flexible and should be easily recognized by the N-end rule-related enzymes. This raised the question of how SUB1A-1 can escape N-end rule regulation.

Our assays (Fig. 7A and 7B) showed that C-terminally truncated SUB1A-1 could be degraded via N-end rule pathway, suggesting that the C-terminus of SUB1A-1 is involved in inhibiting its degradation. Yeast-two hybrid and iTC experiments showed the physical interaction between N- and C-termini of SUB1A-1 (Fig. 7C and 7D). Hence, it is likely that C-terminus of SUB1A-1 helps mask the N-terminal region involved in the N-end rule pathway. An analogous scenario has been reported for the α-synclein protein, where long-range interdomain interactions lead to stabilization by adopting an ensemble of conformations to mask its amyloidogenic domain (45, 46). Taken together, these results suggest that features in both the N-terminus and C-terminus of SUB1A-1 contribute to its escape from N-end rule degradation, likely through domain-domain interactions that prevent adequate exposure of the N-terminus or block the site of ubiquitination. However, the detailed molecular mechanism remains unclear and requires further investigation.

SUB1A-1 is a major factor that confers submergence tolerance in rice. It is up-regulated not only under submergence, but also during drought, prolonged darkness, oxidative stress, and ethylene stress, and plays a key role in a range of abiotic stress responses in addition to submergence (8, 27, 28, 47, 48). The decoupling of SUB1A-1 from N-end rule regulation may have allowed SUB1A-1 to adopt a wider range of functions as a master transcriptional regulator, functioning as a hub to orchestrate the signaling networks in response to various stresses under either normoxic or hypoxic conditions. However, this raised the question of how rice discriminates the submergence stress (hypoxia) from other *SUB1A-1*-regulated stresses that occur when oxygen is readily available. In this study, we identified *ERF66* and *ERF67*

as direct downstream targets of SUB1A-1 and substrates of the N-end rule pathway, which may be critical for co-ordinating hypoxia-responses. In addition, RNA-seq analyses showed that two distinct groups gene were induced by SUB1A-1, one group is dependent on ERF66 and ERF67 and the other group is independent of ERF66 and ERF67 (Fig. 5 and *SI Appendix*, Dataset S1). SUB1A-1 is a transcription factor involving several important processes under submergence stress (49), our data suggested that *ERF66* and *ERF67* are the downstream genes of SUB1A-1, and these two genes involved several important processes during submergence and confer submergence tolerance to rice as well as *SUB1A-1*. This appears similar to the situation in *Arabidopsis*, where the ERFVIIs *HRE1* and *HRE2* are downstream of RAP2.2, 2.3 and 2.12 (15). We propose that this *SUB1A-1* to *ERF66*/*ERF67* regulatory cascade is the link that allows rice to distinguish between submergence and other abiotic stresses (Fig. 8). In this model, *SUB1A-1* is induced under different abiotic stresses, which in turn activates *ERF66*/*ERF67* genes and a set of common stress response genes. Under normoxic abiotic stress conditions, ERF66 and ERF67 are degraded via the N-end rule pathway. Only under low oxygen conditions would ERF66 and ERF67 be stabilized, accumulating to trigger hypoxic responses, and allowing FR13A and flooding tolerant cultivars to survive up to two weeks under complete submergence. The constitutive stability of SUB1A-1 means that once oxygen levels return to normal after de-submergence, ERF66/67 would be quickly degraded to switch off the specific hypoxia transcriptional response, but SUB1A-1 would remain stable to coordinate the expression of other genes that are needed for de-submergence/ drought/ROS survival.

Materials and Methods

For further details of experimental procedures please see *SI Appendix*, *SI Materials and Methods*.

Plant Materials

Rice (*Oryza sativa*) cultivar FR13A, IR29, IR64, Swarna, and Tainung 67 (TNG67) were used in this study. Two near-isogenic lines, IR64(*Sub1*) and Swarna(*Sub1*), were kindly provided by the National Plant Genetic Resources Center of the Taiwan Agricultural Research Institute, Taiwan. SUB1A-1/ERF66/ERF67 overexpression transgenic rice lines (SUB1A-1 OE/ERF66 OE/ERF67 OE) were generated by transforming the *UbiP::GST-SUB1A-1/ERF-66/ERF67* in pCAMBIA1301 vector into TNG67 rice. ERF66 and ERF67 overexpression transgenic *Arabidopsis* lines were generated by transforming the *35S::ERF66/ERF67-GFP* in the pK7FWG2 vector into *Arabidopsis* (*Arabidopsis thaliana*) ecotype Columbia-0 (Col-0). Transformation into *Agrobacterium tumefaceiens* and *Arabidopsis* was performed according to established protocols (50). Rice transformation was done by the Transgenic Plant Core Lab of Academia sinica.

Growth Conditions and Submergence Treatment

Rice seeds were sterilized with 1.2% (v/v) sodium hypochlorite containing 0.1% (v/v) Tween 20 for 30 min and washed at least five times with sterilized water. The sterilized seeds were placed on moist filter paper in petri dishes at 37°C in the dark for 4 days. After incubation, uniformly germinated seeds were transplanted onto an iron grid in a beaker with quarter-strength Kimura B solution, pH 5.6-5.8 (51) and the solution was renewed every two days. The hydroponically cultivated seedlings were grown in a growth chamber at 28°C with a 16-h-light (120-125 $\mu mol \cdot m^{-2} \cdot S^{-1}$)/8-h-dark cycle until they were 14 d old. For submergence treatment of 14-d-old rice seedlings, beakers with plants were placed into a in water tank (W:L:H, 40 cm x 40 cm x 70 cm) filled 55 cm high with tap water for the indicated times at 28°C in dark. For phenotypic assays, data were collected from each genotype in two independent experiments. Fourteen days old seedlings were subjected to submergence treatment as previous described for 7 days in dark. After submergence treatment, the rice seedlings were put back into the growth chamber at 28°C with a 16-h-light (120-125 $\mu mol \cdot m^{-2} \cdot S^{-1}$)/8-h-dark cycle for a further 14 days of recovery, followed by whole plant viability was evaluated. Plants were scored as viable when one or more new leaves appeared during the recovery period.

Protoplast Preparation and Transformation

Rice protoplast preparation and transformation were conducted as described (58, 59) with minor modifications. For protoplast preparation, the stem and sheath of the14-d-old TNG67 rice seedlings were cut into 0.5 mm strips and incubated in an enzyme solution (2% Cellulase RS (Yakult), 1% Macerozyme R10 (Yakult), 0.1% MES at pH 5.6, 0.6 M mannitol, 0.1% $CaCl_2$ and 1% BSA) and vacuum infiltrated (15-20 cm-Hg) for 15 min. After vacuum infiltration, the strips in the enzyme solution were gently shaken under light for about 3.5 hr until the protoplasts were released into the solution. After digestion, the solutions containing protoplasts were filtered through 40 μm nylon meshes, followed by centrifuging at 200 *g* for 3 min with a swinging bucket to pellet the protoplasts in a round-bottomed tube. The supernatants were removed and the protoplast pellets were re-suspended in W5 solution (154 mM NaCl, 125 mM $CaCl_2$, 5 mM KCl, 5 mM glucose, and 2 mM MES at pH5.7) and this step was further repeated once, then protoplasts were incubated and re-suspended on ice for at least 30 min. Then, the W5 solution was removed and protoplasts were re-suspended to a final concentration of 2 to 5 × 10^5 cells/mL in MMG solution (0.6 M mannitol, 15 mM $MgCl_2$, and 4 mM MES at pH5.7). For protoplast transformation, a total of about 4 × 10^5 protoplasts in 0.2 mL of MMG solution were mixed with 20 μg of plasmid DNA on ice for 10 min. Then, an equal volume (about 220 μL) of PEG-calcium solution (40% (w/v) PEG (MW 4000; Sigma), 0.6 M mannitol, and 0.1 M $CaCl_2$) was added, and the mixture was incubated at room temperature for 20 min. After incubation, 3 mL of W5 solution was added slowly and gently mixed, and the protoplasts were pelleted by centrifugation at 200 *g* for 1 min with a swinging bucket. After washing twice with W5 solution, the pellets were re-suspended gently in 1.5 mL of W5 solution and incubated in 6-well plates coated with 1% BSA at room temperature for the indicated times in dark.

Chromatin Immunoprecipitation Quantitative PCR Assay

To detect direct target genes of SUB1A-1, chromatin immunoprecipitation quantitative PCR (ChIP-qPCR) assays were performed by using rice protoplast system. Cross-linking was conducted as described (60) with minor modification. Briefly, *UbiP::SUB1A-1-Luc* constructs and *Ubi::Luc* constructs (as a control) were transfected into TNG67 rice protoplasts, respectively. After 4-hr incubation at room temperature (RT), the transfected protoplasts (1.6 × 10^6 cells per transfection) were collected by centrifugation at 200 *g* for 2 min at RT, followed by removing the supernatants. The collected protoplasts were subjected to cross-linking with 1% formaldehyde in 1.5 mL W5 solution and gently mixed on a rotor (12 rpm) for 10 min at RT. To quench the cross-linking reaction, 80 μL of 2M glycine was added and gently mixed on a rotor (12 rpm) for 5 min at RT, followed by centrifugation at 1500 *g* for 5 min at 4°C to remove the supernatant, and the protoplasts were rinsed with 1 mL of ice-cold 1X PBS buffer (pH 7.4). Chromatin extraction, MNase digestion, sonication, immunoprecipitation, reverse cross-linking, recovering DNA, and qPCR were conducted by using Pierce Magnetic ChIP kit (Thermo Scieientific, Cat. No. 26157). These procedures followed the protocol provided by the manufacturer. The DNA-protein complex was immune-precipitated with ant-Luciferase antibody (Santa Cruz, Cat. No. sc-74548) at a concentration of 5 μg for each IP. The bound DNA fragments were then reversely released and amplified by specific qPCR reaction. The primers used in ChIP-qPCR assay have been listed in *SI Appendix*, Table S1.

***In vitro* Analyses of Protein Stability**

In vitro analyses of protein stability was conducted as described previously (19). A modified version of pTNT (Invitrogen) expression vector, pTNT4xMYC, was generated to perform the *in vitro* analysis, which possesses T7 promoter and SP6 promoter, 5 β-globin leader, ccdB fragment, 4xMYC fragment, T7 terminator sequentially. Firstly, pTNT was double-digested with XhoI and XbaI and gel-eluted to purify the sticky-ended pTNT vector. The pGWB516 plasmid was used as a template to amplify ccdB fragments carrying XhoI and EcoRV site at the 5' and 3' end and 4xMYC fragments carrying EcoRV and XbaI site at the 5' and 3' end by PCR, respectively. The primers used herein have been listed in *SI Appendix*, Table S2. Following, the amplified ccdB fragments were double-digested with XhoI and EcoRV, and the amplified 4xMYC fragments were double-digested with EcoRV and XbaI. After gel elution, the ccdB fragment and 4xMYC fragment were co-ligated into the sticky-ended pTNT vectors to generate the pTNT4xMYC. The details on sequence of pTNT4xMYC have been shown in *SI Appendix*, Fig S10. The CDS of *ERF66* and *ERF67* were cloned from cDNA derived from submerged FR13A cDNA, and the ERF66 and ERF67 DNA fragments were subcloned into pTNT4xMYC by Gateway system (Invitrogen) to produce C-terminal MYC-tagged fusions driven by T7 promoter. The CDS of *SUB1A-2* was cloned from cDNA derived from submerged IR29 cDNA, and ligated into the modified pTNT3xHA (19) to produce C-terminal HA-tagged fusions driven by T7 promoter. The pTNT3xHA-SUB1A-1 was from Dr. Daniel J. Gibbs (19). N-terminal mutations were incorporated by changing the forward primer sequences accordingly (*SI Appendix*, Table S2). *In vitro* assays of protein stability were carried out by using rabbit reticulocyte lysate system (Promega, Cat. No. L4960) with the addition of 100 μM cycloheximide (CHX) to block mRNA translation. Reactions were first incubated for 30 min at 30°C to allow protein translation. Following this 30 min period, cycloheximide is added to prevent further translation, and a sample of the reactions is taken immediately (T0), then the following samples were taken at indicated time points before mixing with protein loading dye to terminate protein synthesis. Equal amount of each reaction were subjected to anti-HA/MYC immunoblot analysis. All blots were check for equal loading by Ponceau staining.

Western Blot Analysis and Antibodies

Protein extraction from the transfected rice protoplasts (4 × 10^5 cells per transfection) was conducted as described (61). Protein extraction from the transgenic *Arabidopsis* seedling was conducted described (62). Proteins resolved by SDS-PAGE were transferred to PVDF using a MiniTrans-Blot electrophoretic transfer cell (Bio-Rad). Membranes were probed with primary antibody at the following titres: anti-HA (Sigma-Aldrich; Cat. No. H3663),

1:1000; anti-MYC (Sigma-Aldrich; Cat. No. WH0004609M2), 1:1000; anti-tubulin (Sigma-Aldrich, Cat. No. T5168), 1:5000; anti-GUS (Sigma-Aldrich, Cat. No. G5545), 1:1000; and anti-Luciferase (Santa Cruz, Cat. No. sc-74548), 1:200. HRP conjugated anti-mouse (PerkinElmer, Cat. No. NEF822001EA)/rabbit (Calbiochem, Cat. No. DC03L) secondary antibody was used at a titre of 1:3000. Immunoblots were visualized with enhanced chemiluminescence reagent (SuperSignal West Pico, Thermo Scientific). The relative image intensities were quantified by using ImageJ (https://imagej.nih.gov/ij/).

Protein Expression and Purification

The pET32a-SUB1A-1 and pET32a-SUB1A-1N were transformed into *E. coli* Rosetta (DE3). Recombinant protein expression was induced at O.D. 0.6 by adding 1 mM IPTG at 25°C for 6 hr and harvested by centrifugation at 4,700 *g* for 30 min. Cells were resuspended in lysis buffer A (50 mM HEPES at pH 7.5, 400 mM NaCl and 20 mM imidazole) supplemented with 10 μg/ml of DNase I, 1mg/ml of lysozyme and 1 mM PMSF) and lysed by sonication. The lysate was centrifuged at 20,000 *g* for 30 min and the supernatant was loaded onto a column containing NiNTA resin pre-equilibrated with lysis buffer. The column was washed with 20 column volumes (CV) of lysis buffer followed by 5 CV of wash buffer (50 mM HEPES at pH 7.5, 300 mM NaCl and 50 mM imidazole). Proteins were eluted with elution buffer (50 mM HEPES at pH 7.5, 100 mM NaCl, 500 mM imidazole). After removing thioredoxin tag overnight TEV protease treatment at 4°C, the solution was loaded onto a HiPrep Heparin FF 16/10 column pre-equilibrated with buffer A (50 mM HEPES at pH 7.5, 10 mM β-mercaptoethanol and 5% glycerol) with 100 mM NaCl. After column washing, the protein was eluted with a 0-100% gradient of buffer A with 1M NaCl in 20 CV. The protein containing fractions of the major peak were concentrated and polished using ENrich SEC650 column using buffer A with 300 mM NaCl.

For ^{15}N labeled SUB1A-1 N-terminus, *E. coli* Rosetta (DE3) were cultured in Luria broth until O.D. reached to 1.0 and centrifuged at 4000 *g* for 20 min. Cell pellets were then washed and resuspended in M9 buffer three times. Resuspended cells were recovered in M9 medium with ^{15}N-NH_4Cl as the sole nitrogen source for 1 hr at 37°C prior to overnight induction at 16°C by adding 0.5 mM IPTG.

CD Spectrometry

The Far-UV CD spectra were recorded over a range of 204-260 nm at 25°C using a Jasco J-815 spectrometer (Jasco Spectroscopic Company, Japan). 5.5 μM of SUB1A-1 and 12 μM of SUB1A-1N (both in 5 mM HEPES at pH 7.5 and 100 mM NaCl) were transferred to a 1 mm quartz cuvette prior to data collection. All spectra were buffer-subtracted and smoothed using Spectra Analysis (Jasco, Japan). The results are expressed as the mean residual molar ellipticity.

NMR Spectroscopy

The NMR sample, 200 μL pH 7.0 aqueous buffer solution (90% H_2O/10% D_2O) in a 4 mm O.D. Shigemi tube containing 0.14 mM SUB1A-1N protein, 150 mM NaCl, 25 mM potassium phosphate, 1 mM NaN_3, and 0.1 mM 4,4-dimethyl-4-silapentane-1-sulfonic acid (DSS) as an internal chemical shift standard. All NMR data were collected at 298 K on a Bruker 800 MHz NMR spectrometer (AV800) equipped with a TXI cryogenic probe. Two-dimensional (2D) ^{1}H,^{15}N-HSQC spectra were collected with a Band-selective Excitation Short-Transient (BEST) scheme (63). Acquisition parameters for BEST 2D ^{1}H,^{15}N-HSQC: the center of the N-H proton selective pulses at 8.5 PPM, 0.2 second interscan delay; 512 scans per FID, 256 increments in the ^{15}N dimension were accumulated. Solvent-exposed 2D ^{1}H,^{15}N-HSQC data was collected using the Phase-Modulated CLEAN chemical EXchange (CLEANEX-PM) scheme (64) with a 100 msec exchange mixing, 360 scans per increment, and 128 increments in the ^{15}N dimension. NMR data were processed using the Topspin software (Bruker).

iTC Binding Assays

The iTC experiment was performed on an ITC200 calorimeter (MicroCal Inc.) at 25℃. The measurement buffer consisted of 50 mM HEPES, 100 mM NaCl, 1 mM DTT at pH 8.0. The injection syringe (40 μL) was filled with 1 mM SUB1A-1 N terminus and the sample cell was loaded by 200 μL of 100 uM SUB1A-1 C terminus. First injection (0.3μL) of SUB1A-1 N domain was followed by thirteen injection of 3 μL at stirring speed of 1000μx rpm. The titration value of first injection was not used in data analysis. The best fits to the binding isotherms was obtained by subtracting saturated integral of signal from last point as reference. However, the interaction is relatively weak so thermodynamic parameters (N, ΔH, K_A) could not accurately estimated. All data were plotted and analyzed by Microcal Origin software.

Details of RNA extraction and qRT-PCR, RNA-seq and data analysis, Plasmid construction, *Trans*-activation assay, EMSA, yeast two hybrid assay are described in *SI Appendix*, *SI Materials and Methods*. All of the primers for qRT-PCR and cDNA cloning, and probes for EMSA are listed in *SI Appendix*, Table S1-S3.

Data deposition

The raw sequencing data from this study have been deposited in NCBI BioProject database (https://www.ncbi.nlm.nih.gov/bioproject/) under accession number PRJNA512592.

Author Contributions

M.C.S., M.C.H., and C.C.L. conceived and designed experiments, and then analyzed the data. C.C.L., M.Y.C., Y.R.L., Y.L.W., H.A.Y., H.H., and D.J.G. performed the experiments. H.C.J. and Y.H.H. did recombinant protein expression and purification and conducted CD experiments. S.J.C., Y.T.C, W.C.C., and H.Y.H. performed RNA-seq experiments. D.I. and W.J.W. designed and performed NMR experiments. J.L.W. designed and performed iTC experiments. C.S.L. and F.H.W. did the protoplast transformation. M.C.S., M.C.H., D.J.G., and C.C.L. wrote the manuscript.

Conflict of Interest Statement

The authors declare no conflict of interest.

Acknowledgements

This work was supported by funding from Academia Sinica, Taiwan. We acknowledge the use of the instruments in the Biophysics Core Facility, Scientific Instrument Center at Academia Sinica. The NMR spectra were obtained at the Core Facility for Protein Structural Analysis supported by the National Core Facility Program for Biotechnology. M.C.H. was supported by the Academia Sinica, Ministry of Science and Technology (MOST107-2311-B-001-002) and the Taiwan Protein Project (Grant No. AS-KPQ-105-TPP). D.J.G. was supported by the Biotechnology and Biological Scientific Research Council (grant number BB/M020568/1), and a European Research Council grant (ERC Starting Grant 715441-GasPlaNt). We thank the Plant Tech Core Facility, the NGS Core Facility, the Transgenic Plant Core Lab, and the AS-BSCT greenhouse core facility of Academia Sinica for technical support.

1. Sasidharan R, Voesenek LACJ (2015) Ethylene-mediated acclimations to flooding stress. *Plant Physiol* 169:3-12.
2. Bailey-Serres J, et al. (2012) Making sense of low oxygen sensing. *Trends Plant Sci* 17:129-138.
3. Gibbs J, Greenway H (2003) Mechanism of anoxia tolerance in plant. I. Growth, survival and anaerobic catabolism. *Funct Plant Biol* 30:1-47.
4. Hattori Y, et al. (2009) The ethylene response factors SNORKEL1 and SNORKEL2 allow rice to adapt to deep water. *Nature* 460:1026-1030.
5. Xu K, et al. (2006) *Sub1A* is an ethylene-response-factor-like gene that confers submergence tolerance to rice. *Nature* 442:705-708.
6. Kuroha T, et al (2018) Ethylene-gibberellin signaling underlies adaptation of rice to periodic flooding. *Science* 361:181-186.
7. Singh P, Sinha AK (2016) A positive feedback loop governed by SUB1A1 interaction with mitogen-activated protein kinase3 imparts submergence tolerance in rice. *Plant Cell* 28:1127-1143.
8. Fukao T, Xu K, Ronald PC, Bailey-Serres J (2006) A variable cluster of ethylene response factor-like genes regulates metabolic and developmental acclimation responses to submergence in rice. *Plant Cell* 18:2021-2034.
9. Singh S, Mackill DJ, Ismail AM (2009) Responses of *SUB1* rice introgression lines to submergence in the field: Yield and grain quality. *Field Crops Res* 113:12-23.
10. Nakano T, Suzuki K, Fujimura T, Shinshi H (2006) Genome-wide analysis of the ERF gene family in *Arabidopsis* and rice. *Plant Physiol* 140:411-432.
11. Bui LT, Giuntoli B, Kosmacz M, Parlanti S, Licausi F (2015) Constitutively expressed ERF-VII transcription factors redundantly activate the core anaerobic response in *Arabidopsis thaliana*. *Plant Sci* 236:37-43.
12. Gibbs DJ et al. (2015) Group VII ethylene response factors coordinate oxygen and nitric oxide signal transduction and stress responses in plnats. *Plant Physiol* 169:23-31.
13. Hinz M et al. (2010) *Arabidopsis RAP2.2*: An ethylene response transcription factor that is important for hypoxia survival. *Plant Physiol* 153:757-772.
14. Hess N, Klode M, Anders M., Sauter M (2011) The hypoxia responsive transcription factor genes *ERF71*/*HRE2* and *ERF73*/*HRE1* of *Arabidopsis* are differentially regulated by ethylene. *Physiol Plant* 143:41-49.
15. Licausi F et al. (2010) *HRE1* and *HRE2*, two hypoxia-inducible ethylene response factors, affect anaerobic responses in *Arabidopsis thaliana*. *Plant J* 62:302-315.
16. Park HY et al. (2011) AtERF71/HRE2 transcription factor mediates osmotic stress response as well as hypoxia response in *Arabidopsis*. *Biochem Biophys Res Commun* 414:135-141.
17. Yang CY, Hsu FC, Li JP, Wang NN, Shih MC (2011) The AP2/ERF transcription factor AtERF73/HRE1 modulates ethylene responses during hypoxia in *Arabidopsis*. *Plant Physiol* 156:202-212.
18. Sasidharan R, Mustroph A (2011) Plant oxygen sensing is mediated by the N-end rule pathway: a milestone in plant anaerobiosis. *Plant Cell* 23:4173-4183.
19. Gibbs DJ et al. (2011) Homeostatic response to hypoxia is regulated by the N-end rule pathway in plants. *Nature* 479:415-418.
20. Licausi F et al. (2011) Oxygen sensing in plants is mediated by an N-end rule pathway for protein destabilization. *Nature* 479:419-422.
21. Gibbs DJ et al. (2014a) Nitric oxide sensing in plants is mediated by proteolytic control of group VII ERF transcription factors. *Mol Cell* 53:369-379.
22. Graciet E, Mesiti F, Wellmer F (2010) Structure and evolutionary conservation of the plant N-end rule pathway. *Plant J* 61:741-751.
23. Gibbs DJ, Bacardit J, Bachmair A, Holdsworth MJ (2014b) The eukaryotic N-end rule pathway: conserved mechanisms and diverse functions. *Trends Cell Biol* 24:603-611.
24. Weits DA et al. (2014) Plant cysteine oxidases control the oxygen-dependent brance of the N-end-rule pathway. *Nat Commun* 5:3425.
25. White MD et al. (2017) Plant cysteine oxidases are dioxygenases that directly enable arginyl transferase- catalysed arginylation of N-end rule targets. *Nat Commun* 8:14690.
26. Peña-Castro JM et al. (2011) Expression of rice SUB1A and SUB1C transcription factors in *Arabidopsis* uncover flowering inhibition as a submergence tolerance mechanism. *Plant J* 67:434-446.
27. Fukao T, Yeung E, Bailey-Serres J (2011) The submergence tolerance regulator SUB1A

mediates crosstalk between submergence and drought tolerance in rice. *Plant Cell* 23:412-427.
28. Fukao T, Yeung E, Bailey-Serres J (2012) The submergence tolerance gene *SUB1A* delays leaf senescence under prolonged darkness through hormonal regulation in rice. *Plant Physiol* 160:1795-1807.
29. Jung KH et al. (2010) The submergence tolerance regulator *Sub1A* mediates stress-responsive expression of AP2/ERF transcription factors. *Plant Physiol* 152:1674-1692.
30. Ohme-Takagi M, Shinshi H (1995) Ethylene-inducible DNA binding proteins that interact with an ethylene-responsive element. *Plant Cell* 7:173-182.
31. Sessa, G., Meller, Y. & Fluhr, R. (1995) A GCC element and a G-box motif participate in ethylene-induced expression of the PRB-1b gene. *Plant Mol. Biol.* 28: 145-153.
32. Allen MD, Yamasaki K, Ohme-Takagi M, Tateno M, Suzuki M (1998) A novel mode of DNA recognition by a b-sheet revealed by the solution structure of the GCC-box binding domain in complex with DNA. *EMBO J* 17:5484-5496.
33. Gasch P et al. (2015) Redundant ERF-VII transcription factors bind to an evolutionarily conserved *cis*-motif to regulate hypoxia-responsive gene expression in *Arabidopsis*. *Plant Cell* 28:160-180.
34. Choi WS et al. (2010) Structural basis for the recognition of N-end rule substrates by the UBR box of ubiquitin ligases *Nat Struct Mol Biol* 17: 1175-1181.
35. Matta-Camacho E, Kozlov G, Li FF, Gehring K (2010) Structure basis of substrate recognition and specificity in the N-end rule pathway. *Nat Struct Mol Biol* 17:1182-1187.
36. van Dongen JT, Licausi F (2015) Oxygen sensing and signaling. *Annu Rev Plant Biol* 66:345-367.
37. Mendiondo GM et al. (2016) Enhanced waterlogging tolerance in barley by manipulation of expression of the N-end rule pathway E3 ligase *PROTEOLYSIS6*. *Plant Biotechnol J* 14:40-50.
38. Lasanthi-Kudahettige R et al. (2007) Transcript profiling of the anoxic rice coleoptile. *Plant Physiol* 144:218-231.
39. Tamang BG, Magliozzi JO, Maroof MAS, Fukao T (2014) Physiological and transcriptomic characterization of submergence and reoxygenation responses in soybean seedling. *Plant Cell Environ* 37:2350-2365.
40. van Veen H et al (2014) Group VII ethylene response factor diversification and regulation in four species from flood-prone environments. *Plant Cell Environ* 37:2421-2432.
41. de Marchi R et al (2016) The N-end rule pathway regulateds pathogen responses in plants. *Sci Rep* 6:26020.
42. Vicente J et al (2017) The Cys-Arg/N-end Rule Pathway Is a General Sensor of Abiotic Stress in Flowering Plants. *Curr Biol* 27:3183-3190.
43. Vicente J et al (2018) Distinct branches of the N-end rule pathway modulate the plant immune response. *New Phytol* doi:10.1111/nph.15387.
44. Jisha V et al. (2015) Overexpression of an AP2/ERF type transcription factor OsEREBP1 confers biotic and abiotic stress tolerance in rice. *PLoS One* 10:e0127831.
45. Bertoncini CW, Fernandez CO, Griesinger C, Jovin TM, Zweckstetter M (2005) Familial mutants of α-synuclein with increased neurotoxicity have a destabilized conformation. *J Biol Chem* 280:30649-30652.
46. Ehrnhoefer DE et al. (2008) EGCG redirects amyloidogenic polypeptides into unstructured, off-pathway oligomers. *Nat Struct Mol Biol* 15:558-566.
47. Alpuerto JB, Hussain RMF, Fukao T (2016) The key regulator of submergence tolerance, SUB1A, promotes photosynthetic and metabolic recovery from submergence damage in rice leaves. *Plant Cell Environ* 39:672-684.
48. Tamang BG, Fukao T (2015) Plant adaptation to multiple stresses during submergence and following desubmergence. *Int J Mol Sci* 16:30164-30180.
49. Locke AM, Barding Jr GA, Sathnur S, Larive CK, Bailey-Serres J (2017) Rice SUB1A constrains remodeling of the transcriptome and metabolome during submergence to facilitate post-submergence recovery. *Plant Cell Environ* 4:721-736.